

# The *Virtual Chromaffin Cell*: analyzing $\text{Ca}^{2+}$ transients in active secretory zones.

Allan S. Schneider<sup>a</sup>, Trevor E. Davis<sup>a</sup> and Ion Moraru<sup>b</sup>

*a. Center for Neuropharmacology and Neuroscience, MC136, Albany Medical College, Albany NY.*

*b. Dept. Physiology, University Connecticut School of Medicine, Farmington, CT, USA.*

---

---

**Correspondence:** Dr. Allan S. Schneider, Center for Neuropharmacology and Neuroscience, Albany Medical College, MC136, Albany, NY 12208, USA.  
**Phone** 1-518-262-5837; **Fax:** 1-518-262-5799; **Email:** schneia@mail.amc.edu

*Cell Biology of the Chromaffin Cell*  
R. Borges & L. Gandía Eds.  
Instituto Teófilo Hernando, Spain, 2004

Although the importance of cytosolic  $\text{Ca}^{2+}$  signals in triggering hormone and neurotransmitter release was recognized some four decades ago, there remain critical unresolved issues regarding the dynamics and spatial distribution of the  $\text{Ca}^{2+}$  signal in sub-membrane secretory zones. Because  $\text{Ca}^{2+}$  enters the cell via voltage gated  $\text{Ca}^{2+}$  channels and moves down a steep gradient of four orders of magnitude ( $10^{-3}$  M extracellular to  $10^{-7}$  M cytosolic), its magnitude near exocytotic sites near the mouth of the  $\text{Ca}^{2+}$  channel is difficult to experimentally determine and remains poorly defined. This is due to limitations of spatial and kinetic resolution of experimental cytosolic  $\text{Ca}^{2+}$  measurements in sub-membrane microdomains. Yet it is this active zone  $\text{Ca}^{2+}$  that plays a critical role in evoking vesicle fusion with the plasma membrane and exocytotic secretion. An understanding of the spatio-temporal properties of  $\text{Ca}^{2+}$  signals in sub-membrane secretory zones could provide valuable information about the regulation of these signals, which in turn control the interaction of  $\text{Ca}^{2+}$  with its sensor in the exocytotic machinery.

In the present work we have developed the *Virtual Chromaffin Cell*, (VCC) an advanced, multi-compartment, computational model of  $\text{Ca}^{2+}$  signaling in adrenal chromaffin cells<sup>1</sup>. The model represents a specific application to chromaffin cells of the more general cell modeling software known as the Virtual Cell<sup>2</sup>. The VCC facilitates a quantitative simulation of cytosolic  $\text{Ca}^{2+}$  transients with high spatial (10 nm) and kinetic ( $\leq$  ms) resolution. It thus allows an evaluation of competing cellular processes that control the shape of sub-membrane  $\text{Ca}^{2+}$  transients. Unlike other simulation programs which assume uniform compartment concentrations, the VCC allows for concentration gradients within a compartment, thereby permitting an analysis of cytosolic  $\text{Ca}^{2+}$  gradients in sub-membrane microdomains near sites of exocytosis. These model simulations complement experimental measurements and provide new insights into the  $\text{Ca}^{2+}$  signal regulating secretion.

## RESULTS AND DISCUSSION

In this work we have focused mainly on the fast (sub-second)  $\text{Ca}^{2+}$  transients in active secretory zones near the plasma membrane, which are

relevant to interactions with the Ca<sup>2+</sup> sensor in the exocytosis mechanism. The specific Ca<sup>2+</sup> control systems we have considered include: **a)** Ca<sup>2+</sup> influx during repetitive activation of Ca<sup>2+</sup> channels in various spatial arrays, **b)** diffusion, including sub-cellular diffusional barriers, **c)** binding to mobile and fixed Ca<sup>2+</sup> buffers, including Ca<sup>2+</sup>-binding proteins and charged membrane phospholipids (e.g., PS), **d)** Ca<sup>2+</sup> sequestration by subcellular organelles, and **e)** efflux out of the cell via plasma membrane Ca-ATPase and Na-Ca exchange. Parameters quantifying transport and binding processes were chosen from the experimental literature to the extent possible. We found that the amplitude and kinetics of fast (ms-second), sub-membrane Ca<sup>2+</sup> transients are dominated by the competition between diffusion and endogenous buffering as well as the spatial distribution and rate of repetitive activation of Ca<sup>2+</sup> channels. Organelle Ca<sup>2+</sup> sequestration (e.g., mitochondrial) and plasma membrane efflux mechanisms were slower (seconds – 10's of seconds) and found to contribute to a later phase of decay.

Figure 1 illustrates the effects of the rate of repetitive Ca<sup>2+</sup> channel activation, on the sub-membrane Ca<sup>2+</sup> signal adjacent to the Ca<sup>2+</sup> channel, both in the presence and absence of endogenous Ca<sup>2+</sup> buffers. Two repetitive activation rates were chosen: 3 Hz and 30 Hz. The slower rate is typical of maximal stimulation of chromaffin cells by the physiological transmitter, acetylcholine. The faster activation rate can result from stimuli that impose prolonged depolarization. A uniform array of Ca<sup>2+</sup> channels was chosen with a membrane density of 16 channels/ $\mu^2$ , a channel density close to the upper limit known for chromaffin cells. A fixed endogenous buffer was chosen with a Ca<sup>2+</sup> binding affinity,  $K_d = 10 \mu\text{M}$ , unbinding rate constant,  $k_{off} = 1000 \text{ s}^{-1}$  and buffer concentration of 1 mM.

The top panel in Fig.1 shows that, in the absence of buffer, peak Ca<sup>2+</sup> concentration near the mouth of the Ca<sup>2+</sup> channel can rise to 120  $\mu\text{M}$  in a 3 ms opening of the channel during an action potential, and then rapidly decays back to about 10  $\mu\text{M}$  within 50 ms. Repetitive opening of Ca<sup>2+</sup> channels at a rate of 3/s results in 9  $\mu\text{M}$  increases in the Ca<sup>2+</sup> signal above the previous values with each activation.

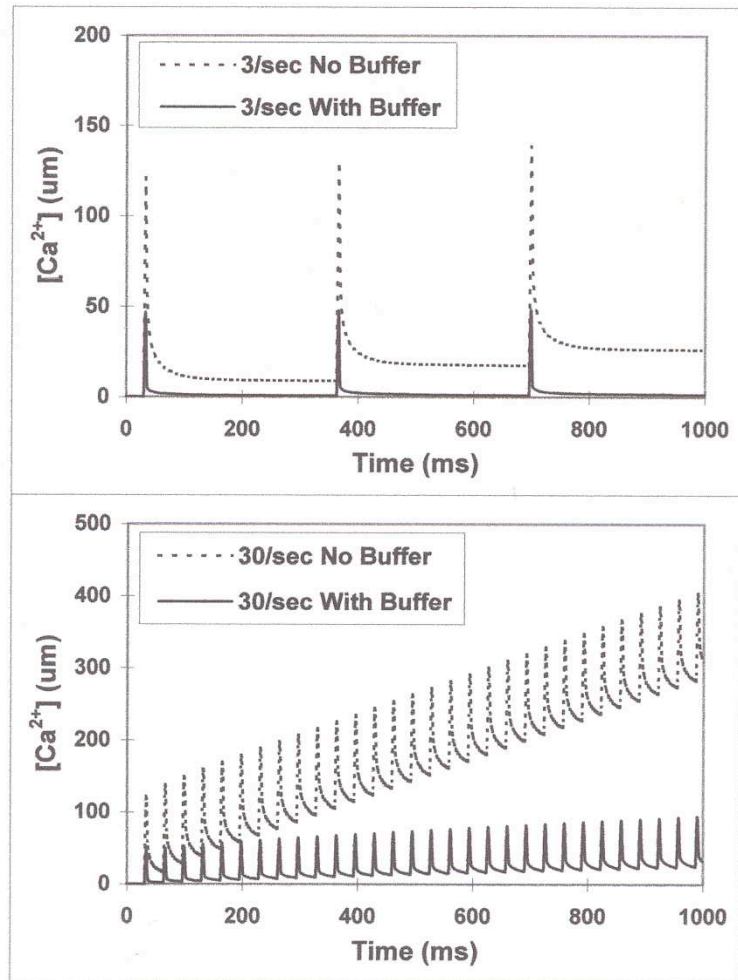


**Figure 1. The effects of repetitive opening of calcium channels and  $Ca^{2+}$  buffering on the  $Ca^{2+}$  signal near mouth of channel. Top panel:** Rate of repetitive channel activation = 3/s. Upper  $Ca^{2+}$  signal curve in the absence of buffer. Lower  $Ca^{2+}$  signal curve in the presence of buffer. Fixed buffer concentration = 1 mM with  $K_d = 10 \mu M$  and  $k_{off} = 1000 s^{-1}$ . **Bottom Panel:** Repetitive channel activation rate of 30/s. Upper curve in absence of buffer; lower curves in presence of same buffer as in top panel. VCC biomodel is radially oriented rectangular rod with  $0.25 \times 0.25 \mu m$  surface membrane and  $8 \mu m$  deep into the cell, with reflecting boundaries, which create the equivalent of a large 2-D array of  $16 channels/\mu^2$ . Single channel current and open time =  $0.3 pA$  and  $3 ms$ , respectively. Computational unit volume element is  $25nm \times 25nm$  in plane of membrane  $\times 80 nm$  depth.

Addition of buffer has a profound effect on the repetitive Ca<sup>2+</sup> signal. Its peak value is lowered to less than 50  $\mu\text{M}$  near the channel mouth and the signal returns close to resting levels (less than 1  $\mu\text{M}$ ) between openings of the channel, such that there is very little increase in signal at the 3 Hz repetitive activation rate.

Increasing the repetitive channel activation rate to 30 Hz dramatically raises the Ca<sup>2+</sup> signal in the absence of buffers (bottom panel in Fig.1). Again the initial peak value is 120  $\mu\text{M}$  and the increase with each activation is about 10  $\mu\text{M}$ . Maintaining the 30 Hz activation rate for 1 second, in the absence of buffers, results in the peak Ca<sup>2+</sup> signal rising to about 400  $\mu\text{M}$ , with trough values between Ca<sup>2+</sup> spikes reaching about 300  $\mu\text{M}$ . Again, the presence of 1 mM of a  $K_d = 10 \mu\text{M}$  fixed buffer substantially limits the rise of the 30 Hz repetitive Ca<sup>2+</sup> signals, such that peak values remain under 100  $\mu\text{M}$  and trough values reach only 25  $\mu\text{M}$  at the end of 1 second of repetitive channel activation. These results provide a clear illustration of the critical importance of both the rate of repetitive channel activation and endogenous Ca<sup>2+</sup> buffers on the Ca<sup>2+</sup> signal in sub-membrane regions near Ca<sup>2+</sup> channels and active secretory zones.

We have also explored the effects on the sub-membrane Ca<sup>2+</sup> signal of a variety of other buffer binding parameters, buffer mobility, diffusion rates, diffusional barriers in the cytosol (e.g., organelles), organelle Ca<sup>2+</sup> sequestration and plasma membrane efflux mechanisms (Na/Ca exchange, Ca-ATPase). The charged phospholipid, phosphatidylserine, was found to have a significant effect in reducing the Ca<sup>2+</sup> signal. Diffusional barriers within 0.5  $\mu\text{m}$  of the channel caused a large increase in the sub-membrane Ca<sup>2+</sup> signal. Altering buffer binding affinity, binding rate constant, concentration or diffusional mobility had a profound effect on the sub-membrane Ca<sup>2+</sup> signal and the distance it penetrated into the cytosol. Higher affinity or concentration of buffers confined the Ca<sup>2+</sup> signal to less than 1  $\mu\text{m}$  from the plasma membrane. The combined results illustrate the utility of the *Virtual Chromaffin Cell* in providing insight into the processes that regulate the sub-membrane Ca<sup>2+</sup> signal for neurohormone secretion. The Virtual Cell is also applicable to analysis of Ca<sup>2+</sup> signaling in other cell types, such as developing neural stem and progenitor cells,

which we have found exhibit anomalous  $\text{Ca}^{2+}$  signals that can influence nervous system development<sup>3</sup>.

### REFERENCES

1. Schneider, A.S., T.E. Davis, and I. Moraru, *The Virtual Chromaffin Cell: Computational Modeling of  $\text{Ca}^{2+}$  Signaling in a Classic Neurosecretory Cell*. Soc Neurosci, 2002. Abstract # **439**:16.
2. Loew, L. and J.C. Schaff, *The Virtual Cell: A software environment for computational cell biology*. Trends Biotech, 2001. **19**:401-406.
3. Atluri, P., et al., *Functional nicotinic acetylcholine receptor expression in stem & progenitor cells of the early embryonic mouse cerebral cortex*. Develop Biol, 2001. **240**:143-156.